




# Expression of glucagon-like peptide 1 receptor in neuropeptide Y neurons of the arcuate nucleus in mice

Yvette Ruska<sup>1</sup> · Anett Szilvasy-Szabo<sup>1</sup> · Dora Kovari<sup>1,2</sup> · Andrea Kadar<sup>1</sup> · Lilla Macsal<sup>3</sup> · Richard Sinko<sup>2,3</sup> · Erik Hrabovszky<sup>4</sup> · Balazs Gereben<sup>3</sup> · Csaba Fekete<sup>1,5</sup> 

Received: 27 February 2021 / Accepted: 2 September 2021 / Published online: 1 October 2021  
© The Author(s), under exclusive licence to Springer-Verlag GmbH Germany, part of Springer Nature 2021

## Abstract

Glucagon-like peptide 1 (GLP-1) and its agonists exert anorexigenic effect at least partly via acting on GLP-1 receptors (GLP-1R) in the arcuate nucleus (ARC). While the anorexigenic, proopiomelanocortin (POMC) neurons of the ARC were shown previously to express GLP-1R, the putative GLP-1R-content of the orexigenic, neuropeptide Y (NPY) neurons remained so far undetected. As GLP-1R is abundant in the ventromedial ARC, where NPY neurons are located; here, we address the possibility that GLP-1 can act directly on the orexigenic NPY system via GLP-1R. Double-labeling immunocytochemistry and in situ hybridization were performed on tissues of adult male mice to detect GLP-1R in NPY neurons. In double-immunolabeled preparations, GLP-1R-immunoreactivity was observed in NPY neurons and in axons ensheathing the majority of NPY neurons. Ultrastructural studies confirmed that GLP-1R-immunoreactivity is associated with the outer membrane of NPY perikarya as well as with axons forming symmetric type, inhibitory synapses on NPY-containing neurons. Double-labeling in situ hybridization experiments demonstrated the expression of GLP-1R mRNA in approximately 20% of NPY mRNA-containing neurons of the ARC. In summary, our data demonstrate the presence of GLP-1R protein and mRNA in NPY neurons of ARC and also reveal the innervation of NPY neurons by GLP-1R-containing inhibitory neurons. These observations suggest that GLP-1 signaling can influence NPY neurons both directly and indirectly. Furthermore, GLP-1 signaling on energy homeostasis appears to involve both direct and indirect effects of GLP-1 on the orexigenic NPY neurons, in addition to the previously known effects via the anorexigenic POMC neuronal system.

---

Yvette Ruska, Anett Szilvasy-Szabo have contributed equally to the work.

---

✉ Csaba Fekete  
fekete.csaba@koki.hu

<sup>1</sup> Laboratory of Integrative Neuroendocrinology, Institute of Experimental Medicine, Szigony Street 43, 1083 Budapest, Hungary

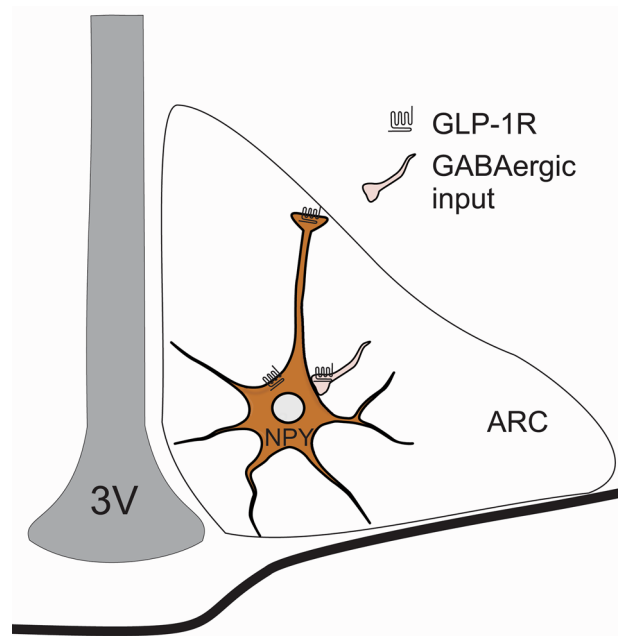
<sup>2</sup> Janos Szentagotthai Doctoral School of Neurosciences, Semmelweis University, 1085 Budapest, Hungary

<sup>3</sup> Laboratory of Molecular Cell Metabolism, Institute of Experimental Medicine, 1083 Budapest, Hungary

<sup>4</sup> Laboratory of Reproductive Neurobiology, Institute of Experimental Medicine, 1083 Budapest, Hungary

<sup>5</sup> Division of Endocrinology, Diabetes and Metabolism, Department of Medicine, Tupper Research Institute, Tufts Medical Center, Boston, MA 02111, USA

## Graphic abstract



**Keywords** Glucagon-like peptide 1 receptor · Neuropeptide Y · Arcuate nucleus · Energy homeostasis

## Introduction

Glucagon-like peptide 1 (GLP-1) is an incretin hormone primarily synthesized by the neuroendocrine L cells of the gut (Baggio and Drucker 2007) and by well-defined neuronal populations of the brain in the nucleus tractus solitarius (NTS) and the intermediate nucleus of medulla oblongata (Larsen et al. 1997; Llewellyn-Smith et al. 2011; Jin et al. 1988). GLP-1 has an important role in the regulation of blood glucose level by increasing the glucose-stimulated insulin secretion, decreasing glucagon secretion and slowing down the gastric emptying (Drucker 2005). GLP-1 also exerts a potent anorexigenic effect by reducing appetite and food intake (Shah and Vella 2014; Yang et al. 2014; Flint et al. 2001). This effect of GLP-1 is mediated at least partly by the central nervous system (Schwartz et al. 2000; Yang et al. 2014).

Due to its anorexigenic and glucose lowering effects, GLP-1 and especially its long-acting analogs are widely used in the therapeutic treatment of type 2 diabetes and obesity (Holst 2004; O'Neil et al. 2018; Astrup et al. 2009). GLP-1 and its analogs exert their effect via a G-protein coupled receptor, the GLP-1 receptor (GLP-1R). In addition to its peripheral appearance, a wide range of studies have demonstrated the extensive distribution of GLP-1R in the central nervous system including brain areas related to food intake and energy expenditure (Merchantaler et al. 1999; Alvarez

et al. 1996; Secher et al. 2014; Farkas et al. 2021; Gabery et al. 2020).

Neurons of the arcuate nucleus (ARC) play pivotal role in the regulation of food intake and glucose homeostasis (Schwartz et al. 2000). The two main energy homeostasis related neuronal groups of the nucleus are the medially located orexigenic neurons expressing agouti-related peptide (AGRP) and neuropeptide Y (NPY) (Zhang et al. 2019), while the more laterally located neurons produce cocaine- and amphetamine-regulated transcript (CART) and proopiomelanocortin (POMC) (Schwartz et al. 2000; Valassi et al. 2008). The POMC neurons have been shown to express GLP-1R (Knudsen et al. 2016; Secher et al. 2014) and GLP-1R agonists were described to exert both direct and indirect effects on these neurons (Peterfi et al. 2020; He et al. 2019; Secher et al. 2014). GLP-1R agonists also influence the NPY/AgRP neurons. Both Exendin-4 and Liraglutide inhibit the firing of these neurons (Secher et al. 2014; He et al. 2019). Liraglutide has been shown to inhibit NPY/AgRP neurons, but this effect was prevented by inhibition of GABA<sub>A</sub> receptors indicating that GLP-1R inhibits the NPY neurons by increasing the activity of pre-synaptic GABAergic neurons (He et al. 2019; Secher et al. 2014). Therefore, it was suggested that the NPY/AgRP neurons do not express GLP-1R and thus the effect of GLP-1 signaling on these neurons is indirect (He et al. 2019). Interestingly, GLP-1R mRNA (Alvarez et al. 1996;

Merchenthaler et al. 1999; Jensen et al. 2018) and pro-tein (Farkas et al. 2021; Jensen et al. 2018) are expressed abundantly in the ventromedial part of the ARC, where the NPY/AgRP neurons are located.

Therefore, here, we revisited the possibility that GLP-1 directly regulates NPY/AgRP neurons, in addition to POMC neurons. To study whether NPY/AgRP neurons of the ARC express GLP-1R, we used double-labeling immunocyto-chemistry at light and electron microscopic levels and dou-ble-labeling in situ hybridization.

## Materials and methods

### Animals

Adult, male FVB/Ant mice ( $N=10$ ) and GLP-1R KO mice ( $N=2$ ) weighing 25–30 g were used. Animals were housed under standard environmental conditions (lights on between 06:00 and 18:00 h, temperature  $22 \pm 1$  °C, mouse chow and water ad libitum). All experimental protocols were reviewed and approved by the Animal Welfare Committee at the Insti-tute of Experimental Medicine.

### Animal and section preparation for immunocytochemistry

To facilitate the visualization of the perikarya of NPY/AgRP neurons with immunocytochemistry, mice ( $N=7$ ) anaesthe-tized with a mixture of ketamine and xylazine (ketamine 50 mg/kg, xylazine 10 mg/kg body weight, intraperitoneally) were intracerebroventricularly injected with 30  $\mu$ g colchicine in 5  $\mu$ l 0.9% saline under stereotaxic control. The colchi-cine treated mice were perfused 1 day after the treatment as described below.

Intact mice ( $N=3$ ) and colchicine-treated mice were tran-scardially perfused with 10 ml 0.01 M phosphate-buffered saline (PBS, pH 7.4), followed by 50 ml mixture of 3% par-aformaldehyde (PFA, Science Services GmbH, München, Germany) and 1% acrolein (Merck, Darmstadt, Germany) in 0.1 M phosphate buffer (PB, pH 7.4). The brains were rapidly removed and postfixed in 4% PFA in 0.1 M PB overnight at room temperature. Serial, 25  $\mu$ m thick coronal sections were cut on a Leica VT 1000S vibratome (Leica Microsystems, Vienna, Austria) through the ARC of the brains. The sections were collected in 0.01 M PBS (pH 7.4) and transferred into anti-freeze solution [30% ethylene gly-col (Cat. # 297, VWR Chemicals, Radnor, PA, USA); 25% glycerol (Cat. # 24,388.295, VWR Chemicals, Radnor, PA, USA); 0.05 M PB] and stored at  $-20$  °C until their use for immunohistochemistry.

### Double-labeling immunofluorescence for NPY and GLP-1R

Every fourth section of three colchicine-treated mice were washed in PBS and incubated in 1% sodium borohydride (Cat. #45,882, Merck, Darmstadt, Germany) in 0.1 M PB for 30 min and then treated with 0.5% Triton X-100 (Cat. # T9284, Merck, Darmstadt, Germany) and 0.5%  $H_2O_2$  (Cat. # 95,321, Merck, Darmstadt, Germany) in 0.01 M PBS for 15 min. After several washing steps in PBS, non-specific antibody binding was blocked with a 2% normal horse serum (NHS) treatment in PBS for 20 min. Then, the sections were incubated overnight in a mixture of primary antibodies: rab-bitized monoclonal antibodies against GLP-1R (0.016  $\mu$ g/ml–0.5  $\mu$ g/ml, Clone 7F38; Novo Nordisk A/S, Copenhagen, Denmark (Farkas et al. 2021)) and sheep antibodies against NPY (1:140,000, gift from I.J. Merchenthaler (Wittmann et al. 2002)) in serum diluent for 2 days at 4 °C. The used rabbitized version of the mouse monoclonal GLP-1R anti-bodies were generated using recombinant technology to graft the heavy and light chain variable regions from the mouse monoclonal antibodies onto a rabbit IgG (Farkas et al. 2021). After several washing steps in PBS, the sections were immersed in a mixture of Alexa 488-conjugated don-key anti-rabbit IgG and Alexa 555-conjugated donkey anti-sheep IgG for 2 h. The sections were mounted onto glass slides and coverslipped with Vectashield mounting medium (Vector Laboratories, Burlingame, CA, USA).

The sections were examined with Zeiss LSM 780 con-focal microscope (Zeiss Company, Jena, Germany) using line by line sequential scanning with laser excitation lines 488 nm for Alexa Fluor 488 and 561 nm for Alexa Fluor 555 with MBS 458/561beamsplitter. The spectral range of each channel was set at 493–558 nm and 566–697 nm for Alexa 488 and Alexa 555, respectively. Plan-Apochromat 20x/0.8 and 63X/1.4 lenses were used. The pinhole size was set at 1 Airy Unit resulting in 2.50 and 0.7  $\mu$ m thin optical slices, respectively. Images were analyzed with Zen 2012 (Zeiss Company, Jena, Germany) and with Adobe Photoshop softwares (Adobe System Inc., Mountain View, CA, USA.).

### Immuno-electron microscopy for NPY and GLP-1R

Sections of four colchicine-treated and three intact mice were washed with PBS and incubated with 1% sodium borohydride in 0.1 M PB for 30 min and then with 0.5%  $H_2O_2$  in PBS for 15 min. The sections were cryoprotected in 15% sucrose in PBS for 30 min at room temperature and in 30% sucrose in PBS overnight at 4 °C, and then quickly frozen over liquid nitrogen and thawed. The freeze–thaw cycle was repeated three times to improve the antibody penetration. The pretreated sections were incubated in 2% normal horse serum (NHS, diluted in 0.1 M PBS) for

20 min to avoid nonspecific antibody binding and then, transferred into a mixture of rabbitized monoclonal antibodies against GLP-1R (0.016 µg/ml, Clone 7F38; Novo Nordisk A/S, Copenhagen, Denmark) and sheep antibodies against NPY (1:140,000, gift from I.J. Merchenthaler) for 4 days at 4 °C. After rinsing in 0.01 M PBS and 0.1% cold water fish gelatin/1% bovine serum albumin (BSA) in PBS, the sections were incubated overnight in donkey anti-sheep IgG conjugated with 0.8 nm colloidal gold (1:100; Electron Microscopy Sciences, Fort Washington, PA, USA), followed by biotinylated donkey anti-rabbit IgG (Jackson ImmunoResearch, West Grove, PA, USA) diluted at 1:500 in 0.01 M PBS containing 0.1% cold water fish gelatin and 1% BSA. After washing, the sections were fixed in 1.25% glutaraldehyde (Electron Microscopy Sciences, Fort Washington, PA, USA) in 0.1 M PB for 10 min at room temperature. Following further rinses in 0.01 M PBS, the sections were washed in Aurion ECS buffer (Aurion, Wageningen, Netherlands, 1:10 dilution with distilled water) for 2 × 10 min. The gold particles labeling NPY were silver intensified with the Aurion R-Gent SE-LM Kit (Aurion, Wageningen, Netherlands) after rinsing in 0.2 M sodium citrate (pH 7.5), followed by treatment in avidin–biotin complex (ABC Elite, PK-6100, 1:1000, Vector Laboratories, Burlingame, CA, USA). GLP-1R-immunoreactivity was detected with following developer: 0.05% DAB/0.15% Ni-ammonium-sulfate/0.005% H<sub>2</sub>O<sub>2</sub> in 0.05 M Tris buffer (pH 7.6).

Upon completion of immunolabeling, the sections were incubated in 1% osmium-tetroxide (Electron Microscopy Sciences, Fort Washington, PA, USA) for 1 h at room temperature, and then treated with 2% uranyl acetate in 70% ethanol for 30 min. Following dehydration in an ascending series of ethanol and acetonitrile (Cat. # 360,457, Merck, Darmstadt, Germany), the sections were flat embedded in Durcupan ACM epoxy resin (Cat. # 44,610, Merck, Darmstadt, Germany) on liquid release agent (Cat. # 70,880,

Electron Microscopy Sciences, Fort Washington, PA, USA)-coated slides, and polymerized at 56 °C for 2 days.

Ultrathin, 60–70 nm thick sections were cut with Leica UCT ultramicrotome (Leica Microsystems, Vienna, Austria). The ultrathin sections were mounted onto Formvar-coated, single slot grids, treated with lead citrate and examined with a JEOL-100 C transmission electron microscope.

### Antibody specificity

Specificity of the antibodies was described elsewhere (Wittmann et al. 2002; Farkas et al. 2021). The specificity of the GLP-1R-immunofluorescence in the ARC was confirmed further by performing immunofluorescent detection of GLP-1R on sections of wild type and GLP-1R KO mice. The GLP-1R-immunoreactivity was completely absent in the ARC of GLP-1R mice (Fig. 1).

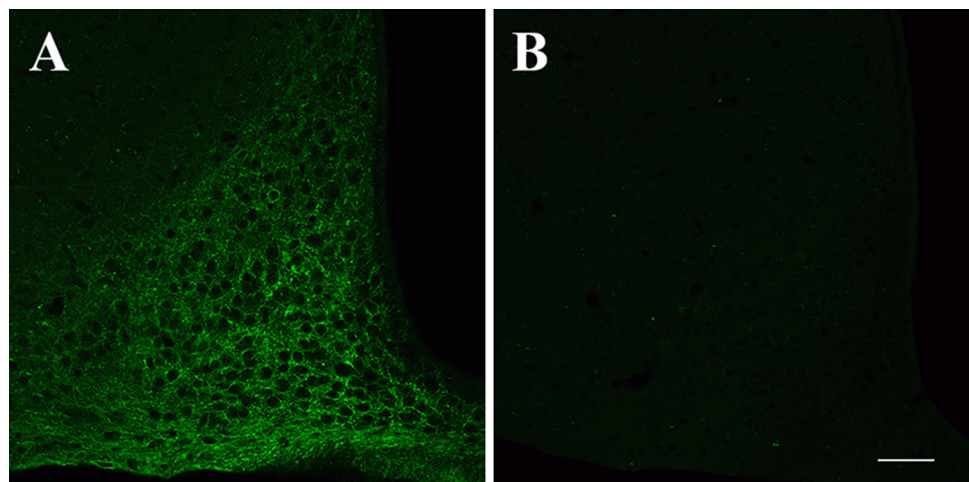
### Dual-labeling in situ hybridization for NPY and GLP-1R mRNAs

Mice ( $N=3$ ) were decapitated. The brains were removed rapidly from the skull, frozen in powdered dry ice and stored at – 80 °C until sectioning.

Serial, 12 µm thick coronal sections were cut through the ARC on a Leica CM 3050 S cryostat (Leica Microsystems, Vienna, Austria), thaw-mounted on gelatin-coated glass slides, air dried at 42 °C and stored at – 80 °C until used for in situ hybridization.

On the day of hybridization, the sections were fixed with 4% paraformaldehyde in PBS (pH 7.4) for 1 h, washed in twofold concentration of standard sodium citrate (2 × SSC), acetylated with 0.25% acetic anhydride in 0.9% triethanolamine for 20 min, and then treated in graded solutions of ethanol (70, 80, 96, and 100%), chloroform, and a descending series of ethanol (100 and 96%) for 5 min each, and hybridized. The hybridization was performed under glass

**Fig. 1** Specificity of the used GLP-1R antibodies. The specificity of the GLP-1R antibodies in the arcuate nucleus were demonstrated by performing immunofluorescent detection of GLP-1R on sections of wild type (a) and GLP-1R KO mice (b). The GLP-1R immunoreactivity was completely absent in the arcuate nucleus of GLP-1R KO mice. *GLP-1R* glucagon-like peptide 1 receptor, *GLP-1R KO* glucagon-like peptide 1 receptor knock-out. Scale bar: 50 µm



coverslips in a buffer containing 50% formamide,  $2 \times$  SSC, 0.25 M Tris (pH 8.0), Denhardt's solution, 10% dextran sulfate, 0.5% sodium dodecyl sulfate, 265  $\mu\text{g}/\text{ml}$  denatured salmon sperm DNA, 40 mM dithiothreitol and digoxigenin-labeled NPY probe diluted 1:100, and  $6 \times 10^5$  cpm of  $^{35}\text{S}$ -labeled GLP-1R cRNA probe. The digoxigenin-labeled antisense NPY cRNA probe was synthesized using a 465 base pair cDNA template corresponding to bases 10–474 of the mouse NPY mRNA coding sequence (GenBank #NM\_023456), while the  $^{35}\text{S}$ -labeled GLP-1R cRNA probe was synthesized using a 1392 base pair long cDNA template corresponding to bases 11–1402 of the mouse GLP-1R coding sequence (GenBank # NM\_021332.2).

After hybridization, the slides were rinsed in  $1 \times$  SSC 3 times and treated with ribonuclease A (25  $\mu\text{g}/\text{ml}$ ; Sigma-Aldrich) in RNase buffer for 1 h at 37 °C, followed by washes in  $1 \times$  SSC (15 min),  $0.5 \times$  SSC (15 min), and  $0.1 \times$  SSC ( $2 \times 30$  min) at 65 °C. Then, the slides were washed in PBS for 10 min, treated in 0.5% Triton X-100 and 0.5%  $\text{H}_2\text{O}_2$  for 15 min and washed in PBS for  $3 \times 10$  min. Then, the slides were washed in 1% BSA dissolved in PBS and incubated in  $F_{\text{ab}}$  fragments of peroxidase-conjugated sheep anti-digoxigenin antibodies (Roche Diagnostics GmbH, Mannheim, Germany, Cat. # 11,207,733,910) diluted 1:100 in 1% bovine serum albumin overnight. Slides were then rinsed in PBS and the NPY hybridization signal was amplified with biotinylated tyramide for 10 min using the TSA amplification kit (Perkin Elmer Life and Analytical Sciences, Waltham, MA, USA) according to the manufacturer's instructions. Slides were rinsed again in PBS and incubated in Alexa 555-conjugated Streptavidin for 2 h diluted 1:250 with 1% BSA in PBS. Slides were then rinsed in PBS, dehydrated in ascending series of ethanol and air dried.

The slides were dipped into Kodak NTB autoradiography emulsion (Carestream Health, Rochester, NY, USA) diluted 1:1 in MQ water and were stored at 4 °C for 42 days. The autoradiograms were developed using EMS Developer D-19 Replacement Kit (Electron Microscopy Sciences, Fort Washington, PA, USA).

After dehydration in ascending series of ethanol and xylene, the slides were coverslipped with DPX mounting medium. Darkfield and fluorescent images were captured through  $20 \times$  or  $40 \times$  objective with Zeiss AxioImager.M1 microscope equipped with AxioCam MRC5 (Carl Zeiss, Gottingen, Germany) and using AxioVision Se64 Rel.4.9.1 software. The images were overlaid using Adobe Photoshop (Adobe System Inc., CA, USA.).

To determine the ratio of double-labeled NPY neurons, the silver grains over the NPY neurons were quantitated as described earlier (Hrabovszky et al. 2006). Digital photomicrographs were taken from both sides of the ARC using  $20 \times$  objective from three different anterior–posterior levels of the nucleus. The photographs of the fluorescent and

autoradiographic signals were overlaid in Adobe Photoshop software. The area of each NPY neurons was selected based on the fluorescent signal using the magnetic lasso tool and the area of the cell was copied from the autoradiogram layer and aligned in separate layers of a new Photoshop (PSD) file on white gray background. The files containing the autoradiogram of all NPY neurons of an ARC section were opened with the Image J image analysis software. The area of each cell was measured. Then the threshold was set to highlight the silver grains, but to exclude background. The integrated density of silver grains was measured over each cell separately and was divided by the area of the cell. In addition, the integrated density of silver grains was measured over three regions of the section, where only background signal was detected, and this integrated density was divided by the total area of the measured region. An NPY cell was considered to contain GLP-1R mRNA if the integrated density of silver grains/area of a cell was at least 20 times higher than the same value of the background area. The ratio of the double labeled cells in the different rostro-caudal levels of the ARC was compared using repeated measures ANOVA.

## Results

### GLP-1R immunoreactivity is associated with the NPY neurons in the hypothalamic arcuate nucleus

Double-labeling immunocytochemistry for NPY and GLP-1R demonstrated an abundance of GLP-1R-immunoreactivity in the ventromedial part of the ARC, where the NPY neurons reside. Confocal microscopic examination of the double-labeled preparations showed that GLP-1R-immunoreactivity is associated with the surface of the majority of NPY neurons (Fig. 2a–f). In some NPY neurons, GLP-1R immunoreactivity was also observed inside the cytoplasm (Fig. 2e, f).

### GLP-1R-immunoreactivity is present both on the surface of NPY neurons and in axons innervating the NPY neurons

As GLP-1R was observed on the surface of ARC neurons and also in axons innervating these cells (Farkas et al. 2021), the resolution of confocal microscopy was not sufficient to distinguish between presynaptic and postsynaptic GLP-1R. Therefore, the ultrastructural localization of GLP-1R-immunoreactivity was studied in and around the NPY neurons. GLP-1R-immunoreactivity was observed in association with the outer cell membrane of NPY-containing neurons (Fig. 3a). GLP-1R-immunoreactivity was also associated with the endoplasmic reticulum of these cells (Fig. 3a), likely revealing the site of GLP-1R translation in

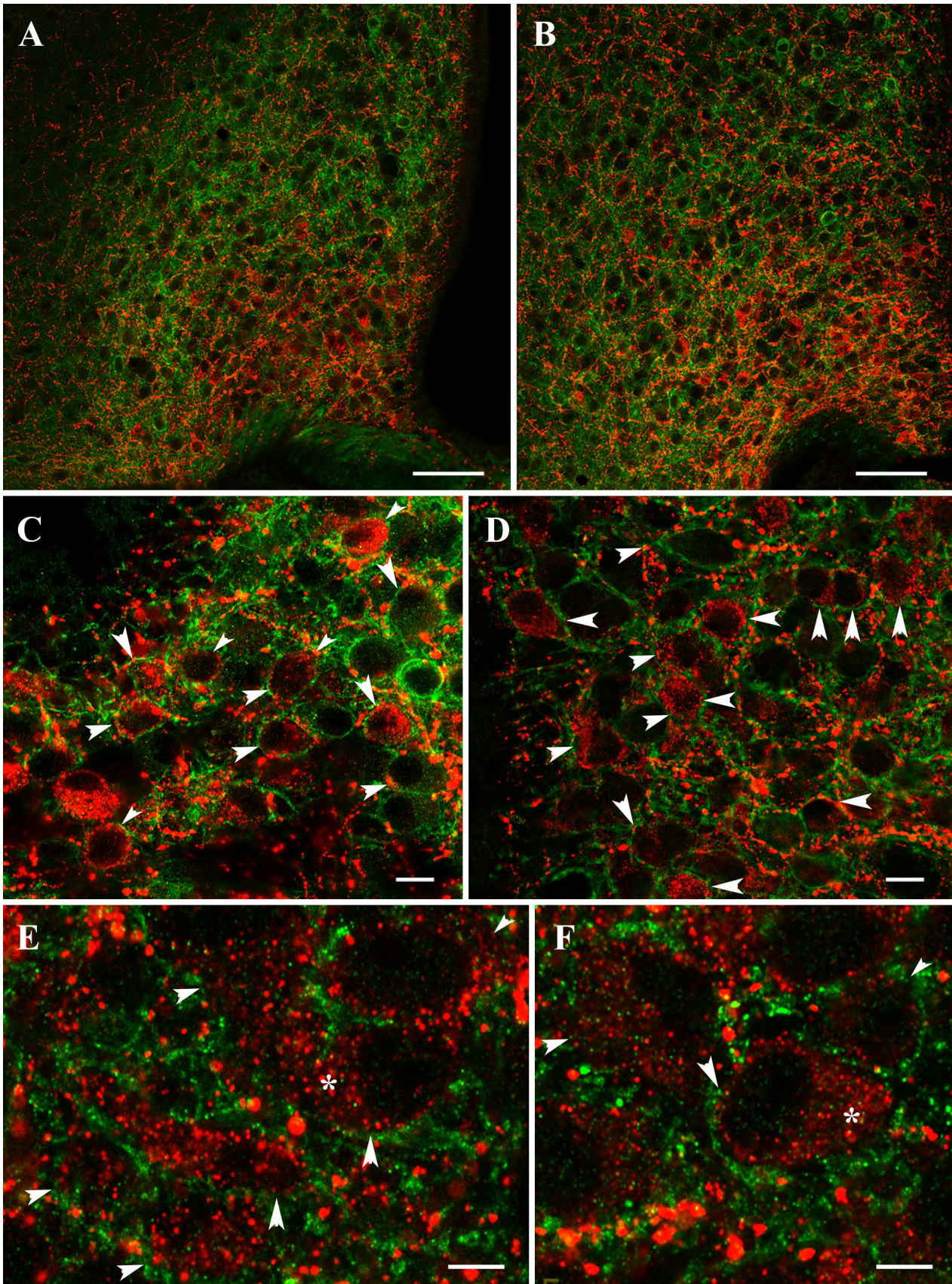


**Fig. 2** Association of GLP-1R immunoreactivity to the NPY neurons of the hypothalamic arcuate nucleus. Double-labeling immunofluorescence for NPY (red) and GLP-1R (green) illustrates the dense GLP-1R immunoreactive network in the ventromedial part of the rostral (a) and caudal (b) parts of the arcuate nucleus, where NPY neurons reside. Higher magnification images illustrate the large number of NPY-immunoreactive perikarya encircled by GLP-1R-immunoreactivity (arrowheads) both in the retrochiasmatic area (c) and in the arcuate nucleus (d). High magnification images (e, f) demonstrate that the GLP-1R-immunoreactivity completely ensheathes the NPY neurons (arrowheads). The GLP-1R immunoreactivity is also detectable in the cytoplasm of some NPY neurons (e, f, stars). Scale bars: 50  $\mu$ m on (a, b) 10  $\mu$ m on (c, d) and 5  $\mu$ m on (e, f)

the NPY neurons. Furthermore, GLP-1R-immunoreactivity was also observed in NPY-containing axons (Fig. 3b), indicating that the receptor is present not only on the perikarya, but also on the projecting axons of NPY neurons.

In addition to the membrane localization of GLP-1R-immunoreactivity on the surface of the NPY neurons, the receptor signal was also observed in association with axons innervating the NPY neurons (Fig. 3c). GLP-1R immunoreactivity was detectable mostly on the outer cell membrane of these axons. GLP-1R axons formed symmetric type synapses on the NPY neurons. GLP-1R was also detected in association to the perikarya of NPY neurons when the mice were not treated with colchicine (Fig. 3d). These findings suggest that GLP-1 signaling may regulate the NPY neurons by both direct effect and indirect effect via presynaptic regulation of the inhibitory inputs of NPY neurons.

### The presence of GLP-1R mRNA in a population of NPY neurons in the ARC

To provide further support for the synthesis of GLP-1R in the NPY neurons of the ARC, double-labeling *in situ* hybridization was performed. The distribution of GLP-1R mRNA was as described earlier (Merchenthaler et al. 1999; Graham et al. 2020). Strongly labeled clusters of silver grains denoting the GLP-1R mRNA hybridization signal were frequently observed dorsal and lateral to the NPY neurons in the ARC. Although, the hybridization signal was weaker in the ventromedial part of the ARC, where the NPY neurons reside, clusters of silver grains were also observed over a population of NPY neurons. Quantification of the double labeled, GLP-1R mRNA containing NPY neurons, showed that  $20.69 \pm 4.7\%$  of NPY neurons express GLP-1R mRNA in the ARC. When the different rostro-caudal levels of the ARC were separately analyzed  $16.97 \pm 7.05\%$ ,  $14.30 \pm 2.52\%$  and  $30.81 \pm 5.84\%$  of NPY neurons was observed to express GLP-1R mRNA in the rostral, mid and caudal regions of the ARC, respectively. The ratio of colocalization had a strong tendency to be higher in the caudal ARC ( $P=0.054$ ) (Fig. 4).

## Discussion

Long acting GLP-1R agonists improve glucose homeostasis in type 2 diabetic patients and induce weight loss in obese patients (Astrup et al. 2009; Holst 2004; O'Neil et al. 2018; Guo 2016). These effects are at least partly mediated by central GLP-1R (Sisley et al. 2014; Candeias et al. 2015; Gabery et al. 2020). The ARC contains high level of GLP-1R (Farkas et al. 2021; Secher et al. 2014; Heppner et al. 2015; Merchenthaler et al. 1999) and plays critical role in the regulation of both the glucose and energy homeostasis (Secher et al. 2014; Heppner et al. 2015). A number of previous studies demonstrated that GLP-1R is synthesized by the anorexigenic POMC neurons of this nucleus (Peterfi et al. 2020; Knudsen et al. 2016), but failed to detect this receptor in the NPY/AgRP neurons using immunocytochemistry and fluorescent *in situ* hybridization methods (He et al. 2019; Secher et al. 2014).

Intriguingly, however, using isotopic *in situ* hybridization, Merchenthaler et al. (Merchenthaler et al. 1999) showed large number of GLP-1R mRNA-containing neurons in the ventromedial part of the ARC, where the NPY neurons are located (Pelletier et al. 1984). GLP-1R expressing neurons were also detected in this subdivision of the ARC in GLP-1R-CRE-eYFP transgenic mice (Cork et al. 2015) and using immunocytochemistry (Farkas et al. 2021; Jensen et al. 2018). These data raised the possibility that GLP-1R might be synthesized by the orexigenic NPY/AgRP neurons in this nucleus.

In agreement with these data, we observed GLP-1R-immunoreactivity in the retrochiasmatic area and in the ventromedial part of the ARC around the NPY neurons using double-labeling immunofluorescence. By confocal microscopy, we observed that the surface of the NPY neurons were ensheathed by GLP-1R-immunoreactivity. Our earlier ultrastructural studies (Peterfi et al. 2020; Farkas et al. 2021) demonstrated the presence of GLP-1R on the surface of ARC neurons, but also on axons innervating ARC neurons. As the used antibodies recognize the extracellular part of the GLP-1R (Jensen et al. 2018), the resolution of confocal microscopy is not sufficient to determine whether the GLP-1R-immunoreactivity on the surface of NPY neurons is associated to the membrane of NPY neurons or to axons surrounding the NPY neurons.

To solve this issue, double-labeling immuno-electron microscopy was performed. At ultrastructural level, we observed that GLP-1R was associated with the outer cell membrane of the NPY neurons and GLP-1R-immunoreactivity was also detectable on the surface of NPY-containing axons suggesting that GLP-1 signaling may act both on the perikarya and on the axons of NPY neurons. In addition, we also found GLP-1R-containing axons that formed

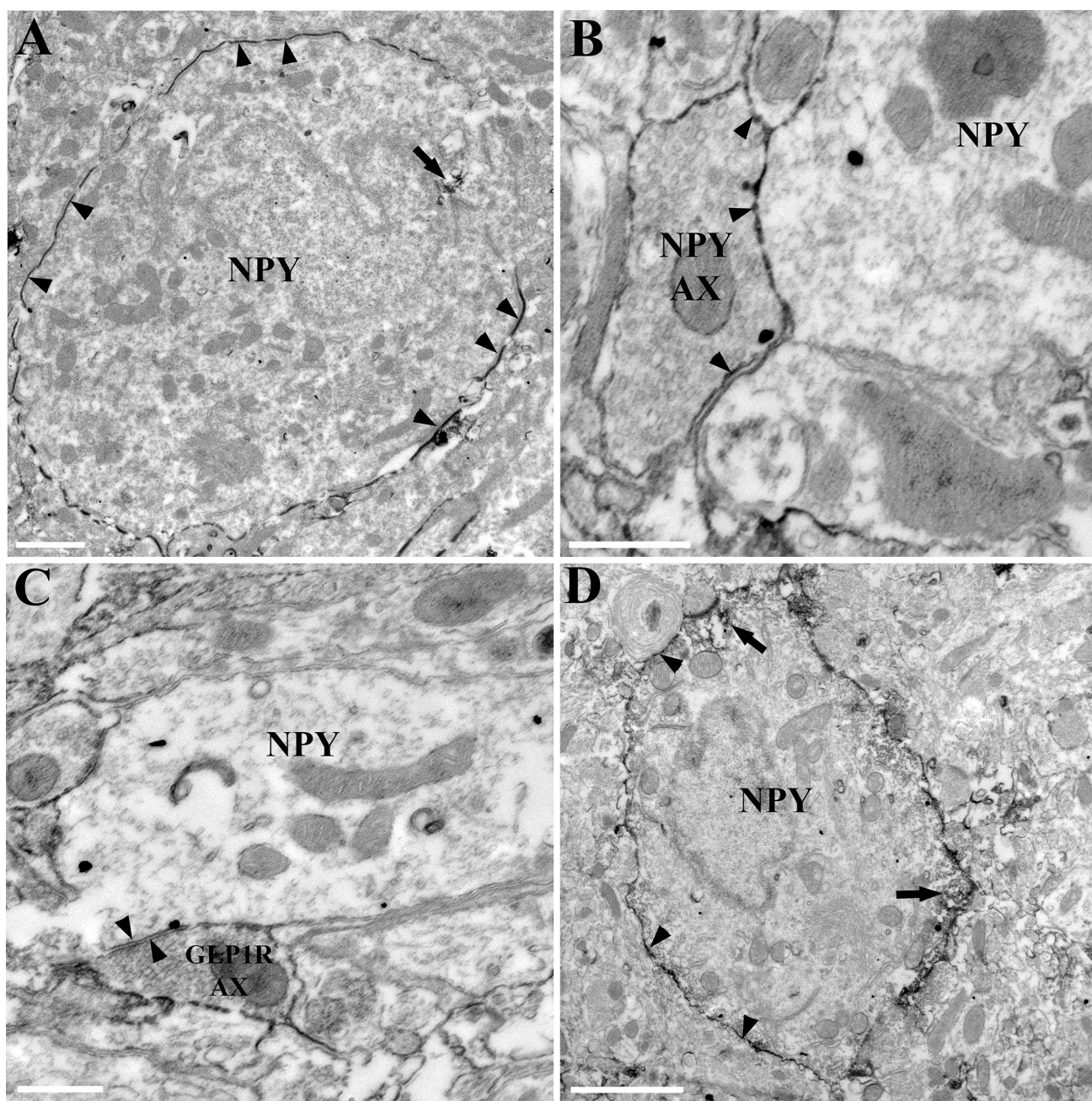


**Fig. 3** Presence of GLP-1R-immunoreactivity in the NPY neurons and the GLP-1R containing innervation of NPY-immunoreactive structures of the arcuate nucleus at ultrastructural level. Electron dense Ni-DAB chromogen labeling the GLP-1R-immunoreactivity is associated to the outer cell membrane (**a**, arrowheads) of an NPY-immunoreactive neuron labeled by highly electron dense silver-intensified gold particles. GLP-1R-immunoreactivity is also attached to the endoplasmic reticulum of NPY neuron (arrow). GLP-1R-immuno-

reactivity (arrowheads) is associated with the surface of an NPY-IR axon (**b**). A GLP-1R-IR axon forms symmetric type synapse on the surface of an NPY-IR dendrite (**c**). Strong GLP-1R-immunoreactivity is also detected in association with the surface (arrowheads) and inside of the cytoplasm (arrows) of NPY neurons without colchicine treatment (**d**). Scale bars: 1  $\mu\text{m}$  on (**a**), 500 nm on (**b**, **c**), and 2  $\mu\text{m}$  on (**d**). AX axon

synapses on NPY-containing neurons. The synapses between the GLP-1R immunoreactive (GLP-1R-IR) axons and the NPY neurons were always symmetrical, indicating inhibitory neurotransmission (Harris and Weinberg 2012).

Thus, the presence of GLP-1R on the perikarya of NPY neurons and on axons innervating these cells suggest that GLP-1 signaling can influence NPY neurons both directly and indirectly.



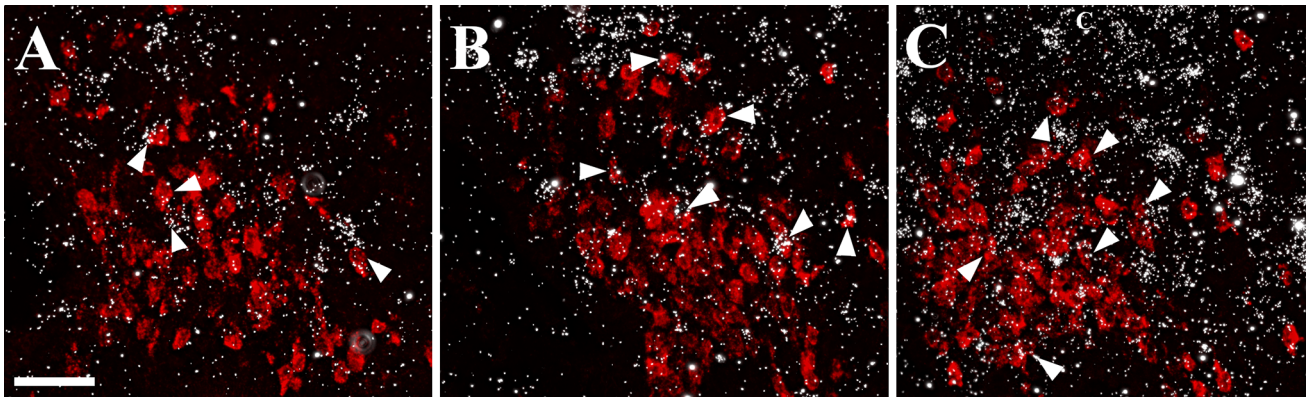


**Fig. 4** Dual-labeling in situ hybridization for NPY and GLP-1R. Double-labeling in situ hybridization revealed that clusters of silver grains denoting GLP-1R mRNA (white dots) overlap with location of the fluorescently labeled NPY mRNA (red) in the arcuate nucleus of

the hypothalamus. The images illustrate double-labeled cells (arrowheads) in the rostral (a), mid (b) and caudal (c) levels of the ARC. The number of double-labeled cells is higher in the caudal part of the nucleus (c). Scale bar: 25  $\mu$ m

To further support the expression of GLP-1R in the NPY neurons, double-labeling in situ hybridization was performed. Results of these experiments confirmed GLP-1R biosynthesis by a population of NPY neurons in the ARC.

Although our data contradict earlier publications showing the lack of GLP-1R in the NPY neurons (He et al. 2019; Secher et al. 2014), the absence of GLP-1R-immunoreactivity in the ARC of GLP-1R KO mice indicates that the immunocytochemical detection of GLP-1R in our study is specific. Furthermore, this labeling specificity is strengthened further by the demonstration of GLP-1R mRNA synthesis in a population of NPY neurons. Therefore, lack of previous evidence for GLP-1R synthesis in NPY neurons was likely due to the lower detection sensitivity.

Some publications also supported the absence of GLP-1R in the NPY neurons by electrophysiological experiments (He et al. 2019; Secher et al. 2014). Secher et al. (2014) observed that GLP-1 triggers outward current in the NPY neurons that can be prevented by GABA<sub>A</sub> antagonist. This observation led to the conclusion that the NPY/AgRP neurons can only be inhibited indirectly by GLP-1 via the mediation of GABAergic neurons. Thus, the authors rejected the possibility of the direct regulation of NPY/AgRP neurons by GLP-1 (Secher et al. 2014). He et al. (2019) also observed that the GLP-1R agonist Liraglutide induces marked inhibition of NPY neurons that is prevented by GABA<sub>A</sub> receptor antagonist. These authors also agreed that the inhibitory effect of GLP-1 on the NPY neurons is mediated by presynaptic GABAergic neurons (He et al. 2019).

Earlier, we showed (Peterfi et al. 2020) that activation of GLP-1R has direct facilitatory effect on presynaptic terminals. Therefore, our observation demonstrating that GLP-1R-IR terminals form inhibitory synapses on NPY neurons also supports the view that GLP-1 signaling can

inhibit the NPY neurons by acting on presynaptic GABAergic terminals.

However, the above mentioned electrophysiological data do not exclude the possibility that GLP-1 can also act directly on the NPY neurons. For example, GLP-1 might induce the synthesis of retrograde signaling molecules within NPY neurons which may, in turn, increase presynaptic GABA release onto NPY neurons.

Similarly, the absence of a direct GLP-1 effect on the membrane potential of NPY neurons does not rule out the possibility of direct GLP-1 signaling. For example, nerve growth factor markedly facilitates the effect of bradykinin on the membrane potential of cultured sympathetic neurons, but alone has no effect on the membrane potential of these cells (Vivas et al. 2014). Similarly, thyrotropin-releasing hormone can prevent the urocortin 3 induced depolarization of POMC neurons without influencing the membrane potential of these neurons when administered alone (Peterfi et al. 2018).

It is also possible that GLP-1 signaling influences the gene expression without altering the electric activity of NPY neurons, thereby inducing long-term changes in the activity and/or responsiveness of NPY neurons.

Functional characterization of GLP-1R signaling on NPY neurons will require further electrophysiological and physiological studies, including the use of NPY cell specific GLP-1R KO animal model.

## Conclusions

In summary, our results demonstrate the presence of GLP-1R mRNA and protein in a population of NPY neurons indicating that GLP-1 signaling can exert direct effect on these neurons. Furthermore, we also showed that the NPY neurons are innervated by GLP-1R-containing inhibitory

axon terminals supporting the view that GLP-1 signaling can inhibit the NPY neurons by facilitating their inhibitory inputs. Further studies will be necessary to determine the importance of the GLP-1R synthesis of NPY neurons in the regulation of glucose and energy homeostasis.

**Acknowledgements** The authors would like to express their appreciation to Andrea Juhász and Veronika Penksza for their great technical assistance.

**Author contributions** YR performed immunohistochemical, ultrastructural and in situ hybridization studies, contributed to data analysis. AS-S performed ultrastructural studies, analyzed data and was involved in the preparation of manuscript. DK was involved in the in situ hybridization studies. AK was involved in the ultrastructural studies. LM, RS, EH and BG generated the probes for in situ hybridization. CF planned and oversaw the experiments, interpreted data and was involved in the preparation of the manuscript.

**Funding** This work was supported by Grants from the Hungarian Science Foundation (OTKA K124767 and K128317), Hungarian National Brain Research Program (2017–1.2.1-NKP-2017–00002), EU H2020 THYRAGE no. 666869.

**Availability of data and materials** Not applicable.

**Code availability** Not applicable.

## Declarations

**Conflicts of interest** C.F. received funding from Novo Nordisk A/S. Y.R., A.Sz-Sz., D.K., A.K., L.M., R.S., E.H., and B.G. declare no competing interest.

**Ethics approval** All experimental protocols were reviewed and approved by the Animal Welfare Committee at the Institute of Experimental Medicine. The study was performed in accordance with the ethical standards as laid down in the 1964 Declaration of Helsinki and its later amendments.

**Consent to participate** Not applicable.

**Consent for publication** Not applicable.

## References

- Alvarez E, Roncero I, Chowen JA, Thorens B, Blazquez E (1996) Expression of the glucagon-like peptide-1 receptor gene in rat brain. *J Neurochem* 66(3):920–927. <https://doi.org/10.1046/j.1471-4159.1996.66030920.x>
- Astrup A, Rossner S, Van Gaal L, Rissanen A, Niskanen L, Al Hakim M, Madsen J, Rasmussen MF, Lean ME, Group NNS (2009) Effects of liraglutide in the treatment of obesity: a randomised, double-blind, placebo-controlled study. *Lancet* 374(9701):1606–1616. [https://doi.org/10.1016/S0140-6736\(09\)61375-1](https://doi.org/10.1016/S0140-6736(09)61375-1)
- Baggio LL, Drucker DJ (2007) Biology of incretins: GLP-1 and GIP. *Gastroenterology* 132(6):2131–2157. <https://doi.org/10.1053/j.gastro.2007.03.054>
- Candeias EM, Sebastiao IC, Cardoso SM, Correia SC, Carvalho CI, Placido AI, Santos MS, Oliveira CR, Moreira PI, Duarte AI (2015) Gut-brain connection: the neuroprotective effects of the anti-diabetic drug liraglutide. *World J Diabetes* 6(6):807–827. <https://doi.org/10.4239/wjd.v6.i6.807>
- Cork SC, Richards JE, Holt MK, Gribble FM, Reimann F, Trapp S (2015) Distribution and characterisation of Glucagon-like peptide-1 receptor expressing cells in the mouse brain. *Mol Metab* 4(10):718–731. <https://doi.org/10.1016/j.molmet.2015.07.008>
- Drucker DJ (2005) Biologic actions and therapeutic potential of the proglucagon-derived peptides. *Nat Clin Pract Endocrinol Metab* 1(1):22–31. <https://doi.org/10.1038/ncpendmet0017>
- Farkas E, Szilvasy-Szabo A, Ruska Y, Sinko R, Rasch MG, Egebjerg T, Pyke C, Gereben B, Knudsen LB, Fekete C (2021) Distribution and ultrastructural localization of the glucagon-like peptide-1 receptor (GLP-1R) in the rat brain. *Brain Struct Funct* 226(1):225–245. <https://doi.org/10.1007/s00429-020-02189-1>
- Flint A, Raben A, Ersboll AK, Holst JJ, Astrup A (2001) The effect of physiological levels of glucagon-like peptide-1 on appetite, gastric emptying, energy and substrate metabolism in obesity. *Int J Obes Relat Metab Disord* 25(6):781–792. <https://doi.org/10.1038/sj.ijo.0801627>
- Gabery S, Salinas CG, Paulsen SJ, Ahnfelt-Ronne J, Alanentalo T, Baquero AF, Buckley ST, Farkas E, Fekete C, Frederiksen KS, Helms HCC, Jeppesen JF, John LM, Pyke C, Nohr J, Lu TT, Poley-Wolf J, Prevot V, Raun K, Simonsen L, Sun G, Szilvasy-Szabo A, Willenbrock H, Secher A, Knudsen LB (2020) Semaglutide lowers body weight in rodents via distributed neural pathways. *JCI Insight*. <https://doi.org/10.1172/jci.insight.133429>
- Graham DL, Durai HH, Trammell TS, Noble BL, Mortlock DP, Galli A, Stanwood GD (2020) A novel mouse model of glucagon-like peptide-1 receptor expression: a look at the brain. *J Comp Neurol* 528(14):2445–2470. <https://doi.org/10.1002/cne.24905>
- Guo XH (2016) The value of short- and long-acting glucagon-like peptide-1 agonists in the management of type 2 diabetes mellitus: experience with exenatide. *Curr Med Res Opin* 32(1):61–76. <https://doi.org/10.1185/03007995.2015.1103214>
- Harris KM, Weinberg RJ (2012) Ultrastructure of synapses in the mammalian brain. *Cold Spring Harb Perspect Biol*. <https://doi.org/10.1101/cshperspect.a005587>
- He Z, Gao Y, Lieu L, Afrin S, Cao J, Michael NJ, Dong Y, Sun J, Guo H, Williams KW (2019) Direct and indirect effects of liraglutide on hypothalamic POMC and NPY/AgRP neurons—implications for energy balance and glucose control. *Mol Metab* 28:120–134. <https://doi.org/10.1016/j.molmet.2019.07.008>
- Heppner KM, Kirigiti M, Secher A, Paulsen SJ, Buckingham R, Pyke C, Knudsen LB, Vrang N, Grove KL (2015) Expression and distribution of glucagon-like peptide-1 receptor mRNA, protein and binding in the male nonhuman primate (*Macaca mulatta*) brain. *Endocrinology* 156(1):255–267. <https://doi.org/10.1210/en.2014-1675>
- Holst JJ (2004) Treatment of type 2 diabetes mellitus with agonists of the GLP-1 receptor or DPP-IV inhibitors. *Expert Opin Emerg Drugs* 9(1):155–166. <https://doi.org/10.1517/eoed.9.1.155.32952>
- Hrabovszky E, Csapó AK, Kalló I, Wilhelm T, Túri GF, Liposits Z (2006) Localization and osmotic regulation of vesicular glutamate transporter-2 in magnocellular neurons of the rat hypothalamus. *Neurochem Int* 48(8):753–761. <https://doi.org/10.1016/j.neuint.2005.12.013>
- Jensen CB, Pyke C, Rasch MG, Dahl AB, Knudsen LB, Secher A (2018) Characterization of the glucagonlike peptide-1 receptor in male mouse brain using a novel antibody and in situ hybridization. *Endocrinology* 159(2):665–675. <https://doi.org/10.1210/en.2017-00812>
- Jin SL, Han VK, Simmons JG, Towle AC, Lauder JM, Lund PK (1988) Distribution of glucagonlike peptide I (GLP-I), glucagon, and glicentin in the rat brain: an immunocytochemical study. *J Comp Neurol* 271(4):519–532. <https://doi.org/10.1002/cne.902710405>

- Knudsen LB, Secher A, Hecksher-Sorensen J, Pyke C (2016) Long-acting glucagon-like peptide-1 receptor agonists have direct access to and effects on pro-opiomelanocortin/cocaine- and amphetamine-stimulated transcript neurons in the mouse hypothalamus. *J Diabetes Investig* 7(Suppl 1):56–63. <https://doi.org/10.1111/jdi.12463>
- Larsen PJ, Tang-Christensen M, Holst JJ, Orskov C (1997) Distribution of glucagon-like peptide-1 and other preproglucagon-derived peptides in the rat hypothalamus and brainstem. *Neuroscience* 77(1):257–270. [https://doi.org/10.1016/s0306-4522\(96\)00434-4](https://doi.org/10.1016/s0306-4522(96)00434-4)
- Llewellyn-Smith IJ, Reimann F, Gribble FM, Trapp S (2011) Preproglucagon neurons project widely to autonomic control areas in the mouse brain. *Neuroscience* 180:111–121. <https://doi.org/10.1016/j.neuroscience.2011.02.023>
- Mercenthaler I, Lane M, Shughrue P (1999) Distribution of pre-proglucagon and glucagon-like peptide-1 receptor messenger RNAs in the rat central nervous system. *J Comp Neurol* 403(2):261–280. [https://doi.org/10.1002/\(sici\)1096-9861\(19990111\)403:2%3c261::aid-cne8%3e3.0.co;2-5](https://doi.org/10.1002/(sici)1096-9861(19990111)403:2%3c261::aid-cne8%3e3.0.co;2-5)
- O'Neil PM, Birkenfeld AL, McGowan B, Mosenzon O, Pedersen SD, Wharton S, Carson CG, Jepsen CH, Kabisch M, Wilding JPH (2018) Efficacy and safety of semaglutide compared with liraglutide and placebo for weight loss in patients with obesity: a randomised, double-blind, placebo and active controlled, dose-ranging, phase 2 trial. *Lancet* 392(10148):637–649. [https://doi.org/10.1016/S0140-6736\(18\)31773-2](https://doi.org/10.1016/S0140-6736(18)31773-2)
- Pelletier G, Desy L, Kerkerian L, Cote J (1984) Immunocytochemical localization of neuropeptide Y (NPY) in the human hypothalamus. *Cell Tissue Res* 238(1):203–205. <https://doi.org/10.1007/BF00215163>
- Peterfi Z, Farkas E, Nagyonyomi-Senyi K, Kadar A, Otto S, Horvath A, Fuzesi T, Lechan RM, Fekete C (2018) Role of TRH/UCN3 neurons of the perifornical area/bed nucleus of stria terminalis region in the regulation of the anorexigenic POMC neurons of the arcuate nucleus in male mice and rats. *Brain Struct Funct* 223(3):1329–1341. <https://doi.org/10.1007/s00429-017-1553-5>
- Peterfi Z, Szilvasy-Szabo A, Farkas E, Ruska Y, Pyke C, Knudsen LB, Fekete C (2020) GLP-1 regulates the POMC neurons of the arcuate nucleus both directly and indirectly via presynaptic action. *Neuroendocrinology*. <https://doi.org/10.1159/000512806>
- Schwartz MW, Woods SC, Porte D Jr, Seeley RJ, Baskin DG (2000) Central nervous system control of food intake. *Nature* 404(6778):661–671. <https://doi.org/10.1038/35007534>
- Secher A, Jelsing J, Baquero AF, Hecksher-Sorensen J, Cowley MA, Dalboge LS, Hansen G, Grove KL, Pyke C, Raun K, Schaffer L, Tang-Christensen M, Verma S, Witgen BM, Vrang N, Bjerre Knudsen L (2014) The arcuate nucleus mediates GLP-1 receptor agonist liraglutide-dependent weight loss. *J Clin Invest* 124(10):4473–4488. <https://doi.org/10.1172/JCI75276>
- Shah M, Vella A (2014) Effects of GLP-1 on appetite and weight. *Rev Endocr Metab Disord* 15(3):181–187. <https://doi.org/10.1007/s11154-014-9289-5>
- Sisley S, Gutierrez-Aguilar R, Scott M, D'Alessio DA, Sandoval DA, Seeley RJ (2014) Neuronal GLP1R mediates liraglutide's anorectic but not glucose-lowering effect. *J Clin Invest* 124(6):2456–2463. <https://doi.org/10.1172/JCI72434>
- Valassi E, Scacchi M, Cavagnini F (2008) Neuroendocrine control of food intake. *Nutr Metab Cardiovasc Dis* 18(2):158–168. <https://doi.org/10.1016/j.numecd.2007.06.004>
- Vivas O, Kruse M, Hille B (2014) Nerve growth factor sensitizes adult sympathetic neurons to the proinflammatory peptide bradykinin. *J Neurosci* 34(36):11959–11971. <https://doi.org/10.1523/JNEUROSCI.1536-14.2014>
- Wittmann G, Liposits Z, Lechan RM, Fekete C (2002) Medullary adrenergic neurons contribute to the neuropeptide Y-ergic innervation of hypophysiotropic thyrotropin-releasing hormone-synthesizing neurons in the rat. *Neurosci Lett* 324(1):69–73. [https://doi.org/10.1016/s0304-3940\(02\)00165-9](https://doi.org/10.1016/s0304-3940(02)00165-9)
- Yang Y, Moghadam AA, Cordner ZA, Liang NC, Moran TH (2014) Long term exendin-4 treatment reduces food intake and body weight and alters expression of brain homeostatic and reward markers. *Endocrinology* 155(9):3473–3483. <https://doi.org/10.1210/en.2014-1052>
- Zhang L, Hernandez-Sanchez D, Herzog H (2019) Regulation of feeding-related behaviors by arcuate neuropeptide Y neurons. *Endocrinology* 160(6):1411–1420. <https://doi.org/10.1210/en.2019-00056>

**Publisher's Note** Springer Nature remains neutral with regard to jurisdictional claims in published maps and institutional affiliations.